Electron transfer during the dissocation of CH3F+ produced by resonant photoemission following F 1s excitation

著者	Prumper G., Carravetta V., Muramatsu Y., Tamenori Y., Kitajima M., Tanaka H., Makochekanwa C., Hoshino M., Liu X. J., Ueda K.
journal or publication title	Physical Review. A
volume	76
number	5
page range	052705
year	2007
URL	http://hdl.handle.net/10097/53588

doi: 10.1103/PhysRevA.76.052705

Electron transfer during the dissociation of CH_3F^+ produced by resonant photoemission following F 1*s* excitation

G. Prümper,[1] V. Carravetta,[1,2] Y. Muramatsu,[1] Y. Tamenori,[3] M. Kitajima,[4] H. Tanaka,[4] C. Makochekanwa,[4,5] M. Hoshino,[4] X. J. Liu,[1] and K. Ueda[1]

[1]*Institute of Multidisciplinary Research for Advanced Materials, Tohoku University, Sendai 980-8577, Japan*

[2]*Institute of Chemical Physical Processes CNR, via Moruzzi 1, 56124 Pisa, Italy*

[3]*Japan Synchrotron Radiation Research Institute, Sayo-gun, Hyogo 679-5198, Japan*

[4]*Department of Physics, Sophia University, Chiyoda-ku, Tokyo 102-8554, Japan*

[5]*Graduate School of Sciences, Kyushu University, Fukuoka 812-8581, Japan*

(Received 21 May 2007; published 9 November 2007)

We present experimental evidence for pronounced electron transfer from C to F^+ happening during the breakup of CH_3F^+ ions in gas phase produced by resonant photoemission following F $1s \rightarrow 6a_1^*$ core excitation of CH_3F. We measured the momentum of the ionic fragments in coincidence with the F *KVV* Auger electrons that show a Doppler shift reflecting the motion of the F nucleus. The correlation between Doppler shift and ion momentum is opposite for the F^+ and the CH_2^+ fragments, indicating that CH_2^+ is produced by electron transfer from C to F^+, after the Auger electron emission from excited moving F. This finding is rationalized by calculations of the potential energy curves of the main states involved in the excitation and decay processes.

DOI: 10.1103/PhysRevA.76.052705 PACS number(s): 34.50.Gb, 07.81.+a, 34.50.Lf, 34.70.+e

Numerous essential processes in chemistry and biology such as corrosion or photosynthesis evolve by electron transfer reactions [1], i.e., an electron moves from one atom or chemical group to another. While typical electron transfer reactions have to be described thermodynamically because they happen between two molecules in solution or between a molecule in a solution and a solid electrode, in this work we will discuss a much simpler case: electron transfer from CH_3 to F^+ during the breakup of CH_3-F^+ in the gas phase. This C-F bond break is a archetypical candidate for electron transfer because the two atoms have very different electronegative character and therefore the CH_3^+-F configuration is lower in energy than the starting configuration CH_3-F^+. For producing CH_3F^+ with the vacancy localized at the F atom, we used the excitation of a F 1*s* electron to the antibonding $6a_1$* orbital, leading to nuclear motion, F *KVV* Auger decay, and fragmentation [2]. High resolution Auger electron-ion momentum coincidence spectroscopy [3,4] is used to prove that the original location of the negative charge was at the moving F atom and to determine the momentum of the ion that is finally produced. Doppler effects in resonant photoemission from molecules undergoing ultrafast dissociation [5] have been observed in many molecules [6–8]. Here we make use of that effect to probe the dynamics during the breakup process of the molecular ion. That is, we use the Doppler shift of each electron to trace the speed of its emitter given by the motion of the core hole orbital. If the Auger decay happens after the dissociation, the valence orbitals involved move together with the core hole and the negative charge produced in the core excited fragment necessarily stays with the emitter of the Auger electron. We will show later that in the decays considered here similar arguments can also be applied for Auger decay happening in the molecular regime. To our knowledge, the present work is the first experimental report on electron transfer during fragmentation being the dominating mechanism for the production of a molecular ionic fragment. The relative simplicity of the reaction allows for a theoretical modeling of all stages of the fragmentation process. In the case of electron transfer happening in solutions, there are solvent molecules with enough fluctuations in their nuclear coordinates to bridge the energy difference between the states before and after the electron transfer. In the present intramolecular reaction, the electron transfer happens nonadiabatically as a jump between two potential energy surfaces describing the electronic states before and after the transfer.

The experimental setup used for recording F *KVV* Auger electrons in coincidence with mass and momentum resolved fragment ions was described in detail elsewhere [4,9], so only a brief account is given here. We used an electron spectrometer at the high resolution photochemistry beamline 27SU [10] at SPring-8 in Japan. A pass energy of 200 eV and an instrumental resolution of about 1 eV were used. The photon energy bandwidth was 100 meV. An ion time-of-flight (TOF) spectrometer was mounted opposite the electron spectrometer inside the vacuum chamber, ions of different masses arriving at different times. The exact time of flight of ions with the same mass contains the information about the ion emission direction: emission in the direction of the ion detector will lead to an earlier detection than emission away from the ion detector. CH_3F was introduced as an effusive beam crossed by the synchrotron radiation. The pressure in the vacuum chamber was 1.5×10^{-4} Pa. During the coincidence experiment, all voltages of the electron spectrometer were fixed, so only electrons in an energy interval from 644 to 659 eV were recorded. The ionizing soft x rays were linearly polarized along the axes of the electron spectrometer and the ion spectrometer.

We calculated diabatic potential curves of the ground state, the core excited state, and the participator and spectator final states, using CAS calculations with a GAMESS-PVTZ basis set, keeping the CH_3 group in the rigid geometry of the ground state, and varying only the C-F bond distance. This simplified model cannot yield accurate values for the kinetic energy release of the fragments nor can it account for C-H

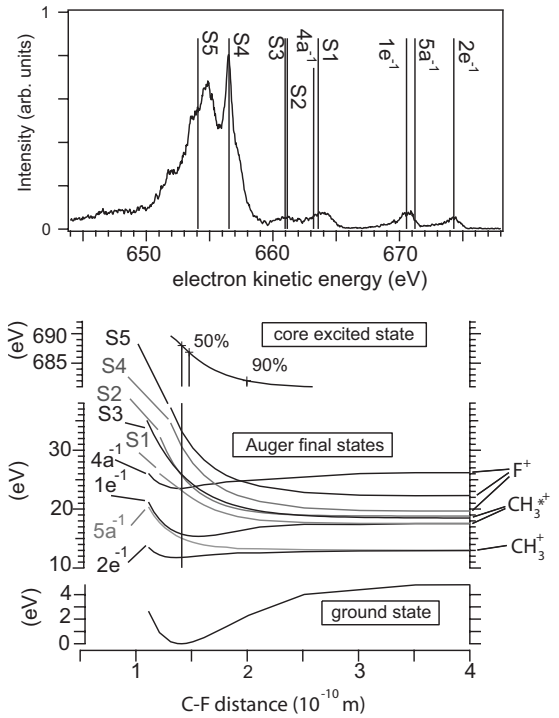

FIG. 1. Upper part: Electron spectrum measured with high resolution [12,13]. The vertical lines show the shifted calculated vertical energies. See the text and Table I for details. The lower part shows the corresponding potential curves of the core excited state, the Auger final states, and the ground state. The labels at the right indicate the ions in the dissociation limit. The vertical lines show the equilibrium distance and the calculated C-F distances where 50% and 90% of the Auger decay have happened.

bond breaks. It can, however, provide an estimate for the dissociation time scale, vertical ionization energies, and the information if the positive charge in the final state stays with the F atom or not. A quite large number of spectator states are present in the considered energy range involving two holes in the valence orbitals $(2e,5a_1,1e,4a_1)$ and one electron in $6a_1(\sigma^*)$, as can be easily understood by considering that for any configuration with three open shells two doublet states are possible and different spatial symmetries can be realized. Such spectator states are often very close in energy and several avoided crossings can be present at different C-F bond lengths among the spectator states as well as with other excited states having different electronic configurations, involving Rydberg orbitals.

Because of this, we present in Fig. 1 and Table I only the most significant spectator (labeled as *S*) and participator diabatic potential energy curves (PECs) for a clearer view. The labels (two valence holes) in Table I refer to the most important configuration(s) contributing to each state at the equilibrium distance R_{eq}. By inspecting the computed wave functions and energy differences we assigned the fragments for large *R* to the curves and put the corresponding labels in Fig. 1.

For the interpretation of the electron spectra it is important to consider that the Auger decay takes place within a few fs after the excitation and therefore close to R_{eq}=1.413 Å,

TABLE I. Auger final states and asymptotic states.

Calculated vertical energy in eV	Shifted	Label and character	Asymptotic ion and ion energy in eV	KER in eV
654.830	654.071	$S5$: $5a1^{-1}$ $1ey^{-1}$	F^+ 4.80	10.876
657.430	656.530	$S4$: $1ex^{-1}$ $1ey^{-1}$	F^+ 4.80	10.876
662.117	660.962	$S3$: $5a1^{-1}$ $2ey^{-1}$ $1ex^{-1}$ $1ey^{-1}$	F and CH_3^{*+} 4.13	7.3884
662.296	661.132	$S2$: $1ex^{-1}$ $2ey^{-1}$ $2ex^{-1}$ $1ey^{-1}$	F and CH_3^{*+} 3.84	6.873
664.495	663.211	$4a^{-1}$	F^+	bound
664.877	663.573	$S1$: $2ex^{-1}$ $2ey^{-1}$	CH_3^{*+} 3.10	5.548
672.255	670.550	$1e^{-1}$	CH_3^{*+}	bound
672.973	671.229	$5a^{-1}$	CH_3^+ 1.12	2.005
676.210	674.290	$2e^{-1}$	CH_3^+	bound

while the ion detection reflects the result of the fragmentation (large *R*) taking place in a longer time. By classical dynamic calculations along the computed potential curve of the core-excited state, assuming a core hole lifetime of 3.5 fs [11], we calculated the internuclear distances where 50% (1.478 Å) and 90% (1.997 Å) of the core hole decay has occurred. The results are shown along the core-excited state PEC in Fig. 1. Only for distances $R>2.0$ Å can the F atom be considered isolated from the CH_3 remainder. Obviously 90% of the decay happens in the molecular regime. The remaining 10% are due to Auger decay occurring for $R>2.0$ Å, where an atomic F^* fragment may decay to the *S*5 state (with the potential surface almost parallel to that of the core excited state).

To get a better agreement with the experiment the PEC of the excited state was shifted to a vertical excitation energy of 688.0 eV. The corresponding transition vertical energies (bars) are compared to the experimental electron spectrum [12,13] shown in the upper panel of Fig. 1. A good correspondence is found when the calculated energy values are scaled and shifted slightly so that lines *S*4 and $2e^{-1}$ coincide with the peaks in the measured spectrum. All shifts are less than 2 eV, as given in Table I. The assignments in Table I and Fig. 1 differ from the ones given in Refs. [2,12] which were based on *ab initio* frozen orbital calculations of the normal Auger spectrum by Liegener [15]. Using the computed PEC, we get the main character of the bands and the fragments produced, if a diabatic fragmentation dynamic is assumed. From the calculated total kinetic energy release, assuming an energy sharing of 15:19 for the F atom and a rigid CH_3 fragment, we calculated the kinetic energy of the ions. The results are given also in Table I.

The coincidence experiment was performed in the limited kinetic energy region containing only the decays to the states *S*4 and *S*5. The main ionic fragments found were H^+, C^+, CH^+, CH_2^+, and F^+. Figure 2 shows the spectra of the electrons recorded in coincidence with these ions. The yield of CH_3^+ was negligible; so was the contribution of double ionization events leading to ion pairs. Apart from H^+, F^+ is the

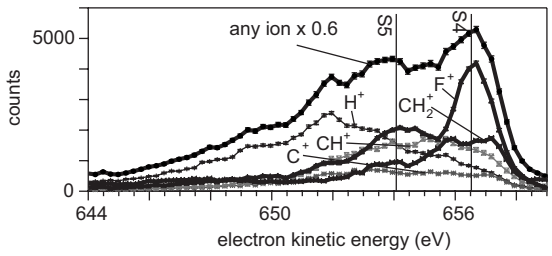

FIG. 2. Spectra of Auger electrons detected in coincidence with different ions.

main ionic fragment, consistent with the fact that only the two bands, *S*5 and *S*4, are present, both leading asymptotically to F^+. H^+, C^+, CH^+, CH_2^+ are not described by our simplified theoretical model, because their production involves one or more C-H bond breaks in addition to the C-F bond break. Nevertheless, we notice that the two electron spectra coincident with F^+ and CH_2^+ are similar in shape, both showing local maxima close to the energies of the states *S*4 and *S*5, indicating that *S*4 and *S*5 are the dominating final states of the Auger decay.

The gray scale maps in Fig. 3 show the correlation of the ion time of flight (i.e., the linear momentum in the direction of the electron detection) and the kinetic energy of the electron, including the Doppler shift. To visualize the Doppler shift more clearly in the upper part of the figure we plotted the spectra of the electrons that belong to the ions emitted towards and away from the electron detector separately. For electrons coincident with F^+ a Doppler shift of 350 meV is observed. The diabatic potential curves predict a kinetic energy of 4.80 eV for the F^+. A fit of the time of flight profile of the F^+ ions detected in coincidence with the electrons in peaks *S*4 and *S*5 correspond to a kinetic energy of 2.4 ± 0.2 eV and an anisotropy of $\beta=1.90\pm0.1$. For CH_2^+ we

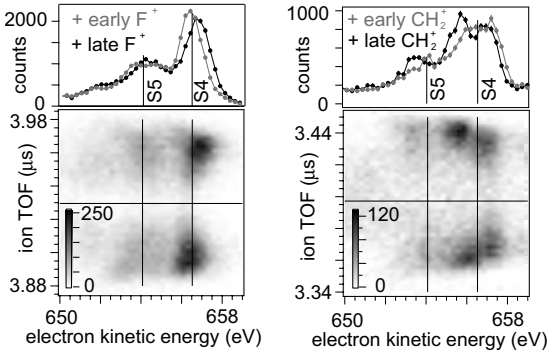

FIG. 3. Lower part: Intensity plots of the time of flight of the ion vs the kinetic energy of the electron detected in coincidence with the ion. Upper part: Spectra of electrons detected in coincidence with an ion emitted in the direction of the electron detector (late ion) and away from the electron detector (early ion). The average shift between the two curves is $+350\pm30$ meV for F^+ and -270 ± 30 meV for CH_2^+. The vertical black lines show the positions of the vertical energies of *S*4 and *S*5, the horizontal black lines show the time of flight of F^+ and CH_2^+ ions with zero kinetic energy.

obtained 4.2 ± 0.2 eV and $\beta=1.20\pm0.1$. We consider the agreement of the value of 4.2 ± 0.2 eV obtained for CH_2^+ with the predicted kinetic energy of 4.13 eV for the CH_3^{*+} fragment in the *S*3 band as coincidence. The theoretical treatment of triple fragmentation is beyond the scope of this work. We cannot explain the discrepancy for the F^+ kinetic energy within our one dimensional model of the nuclear dynamics. The absolute size of the observed Doppler effect of 350 meV is much smaller than the value of 850 meV that belongs to the asymptotic motion (2.4 eV) of F^+ ions. This is understandable, because according to our calculation most of the ion acceleration happens after the Auger decay. On the other hand, 350 meV is much larger than the value of about 100 meV expected from our calculation of the nuclear motion. This indicates that the dissociation is faster or the core hole lifetime is longer than assumed. Probably both effects contribute. A more realistic potential surface for the excited state taking into account the conformation change in CH_3 will lead to a steeper curve and thus more acceleration close to R_{eq}. In the F $1s\rightarrow\sigma^*$ excitation one electron is put into the σ^* orbital that is localized on CH_3. Due to the lower electron density at F compared to core excited atomic F the Auger decay rate might decrease.

For electrons detected in coincidence with CH_2^+ a "negative Doppler shift" of −270 meV is observed. It is smaller, in absolute value, than the one observed for F^+. The negative sign indicates that the electron was not emitted from the CH_2^+ fragment but from F moving in the opposite direction. The smaller absolute value indicates that, in the second case, a smaller kinetic energy was acquired by F at the moment of Auger decay.

As mentioned above, the Auger decay happens mostly in the molecular regime and therefore the mechanism leading to the Doppler effects is much more difficult to understand compared to the atomic regime where the core hole and the valence orbitals all move with the same speed. In the extreme case of molecular Auger decay a moving core hole can be filled by an electron from a delocalized valence orbital $v1$ and an electron from another delocalized valence orbital $v2$ can be emitted. We do not know if in such a situation a Doppler effect in the electron spectrum is possible as an electron is removed from the delocalized orbital $v2$ whose motion may not reflect the motion of the core hole. If it is possible one could observe a similar anticorrelation of the electronic Doppler shift and some fragments produced without assuming a sequence of Auger decay and subsequent electron transfer. A careful analysis of the charge distribution, in core excited CH_3F, of the relevant orbitals around the equilibrium geometry, where the Auger decay mostly occurs, reveals that in the cases considered here the situation is similar to the Auger decay in the atomic regime: the σ^* orbital and the $2e$ orbital are mostly localized on the CH_3 part while the orbitals $5a1$ and $1e$ are mostly localized on the F side. This strong localization is also reflected in the line strengths. The bands *S*4 and *S*5 are stronger than all other bands shown in Table I and Fig. 1. Only for the bands *S*4 and *S*5 both orbitals $v1$ and $v2$ are localized on the F side. In the case of the *S*5 band the $v1$ and $v2$ orbitals are the $5a1$ and $1e$ orbitals, in the case of the *S*4 band, $v2$ and $v2$ are both the $e1$ orbital. Therefore we can safely say that the Auger electron

is emitted from the F fragment. As shown in Table I the localization of the charge stays on the F side as the C-F bond is stretched. In order to localize the charge on the CH_3 side, a transition to states that contain $2e$ contributions is necessary.

We claim that the electrons in peaks $S4$ and $S5$ detected in coincidence with CH_2^+ are due to an Auger decay to the curves $S4$ and $S5$, followed by nuclear and electronic rearrangement involving other curves like $S1$, $S2$, $S3$ yielding excited CH_3^+, or more precisely CH_2^+ after further fragmentation instead of F^+. In our model the electron transfer is interpreted as due to a nonadiabatic transition during the nuclear dynamics, from the $S4$ or $S5$ electronic surfaces to lower, e.g., $S1$, $S2$, or $S3$ surfaces (that yield F instead of F^+). The curves $S1$, $S2$, and $S3$ yield CH_3^+. The energy difference between the upper and lower electronic states with different fragmentation leads to further fragmentation within CH_3^+. During this rearrangement an electron moves from the CH_3 side to the F side. Because electron transfer cannot take place for large C-F distances, it is likely that the CH_2^+ channel probes Auger decay happening at closer C-F distances, where the F fragment is still slow, in agreement with the observed smaller Doppler shift compared to the F^+ channel. Also the angular distribution of CH_2^+ is different from that of F^+ ($\beta=1.20$ instead of $\beta=1.90$). Therefore the distinction between forward and backward ions for CH_2^+ is less sharp than for F^+. This indicates that the C-H bond break and the emission of the H atom deflects the CH_2^+ ion, so its momentum is not exactly opposite to F. The $S4$ band coincident with F^+ is a single peak, while $S4$ electrons coincident with CH_2^+ show not only spectral broadening but also a doublet structure. The time scales of the Auger decay and the proposed electron transfer are similar, as the electron transfer can only happen in a range of C-F distances shorter than the one in which Auger decay may occur. Therefore a strict two step picture is not valid and the second step, the jump from one potential surface to another, can influence the kinetic energy of the Auger electron. The presence of two sets ($S1$) and ($S2,S3$) of potential curves leading to CH_3^{*+} (CH_2^+ and H) with different asymptotic energy values could explain the presence of the $S4$ double peak in the CH_2^+ electron spectrum and the two different kinetic energies of the corresponding CH_2^+ fragments, visible as two spots in Fig. 3. Independent of these speculations about the peak shapes, comparing the overall intensity distribution in the gray scale maps of Fig. 3, one can see very different features. For F^+ the $S5$ peak is broad and the F^+ kinetic energy spread is also broad while the $S4$ peak is sharp. For CH_2^+ it is the opposite: the $S5$ peak is relatively sharp, with a fixed fragment energy while $S4$ is broad (or double structured) with a wide spread of the fragment kinetic energy. This opposite behavior supports the model that the F^+ and CH_2^+ ions originate from the same Auger decays and compete for intensity.

Peaks similar to $S4$ with a kinetic energy close to 656.5 eV were observed for CF_4 and SF_6 [14] as well. Our coincidence measurements on CF_4 and SF_6 showed only weak indications for electron transfer. In this respect CH_3F is an exceptional molecule. There is only one F atom with a strong electronegativity attracting an electron from the less electronegative remainder.

We have performed an electron-momentum-resolved ion coincidence measurement for the F *KVV* Auger electron emission from CH_3F following the F $1s \rightarrow a_1^*$ excitation. We found that the electronic spectra that belong to the two ionic fragments F^+ and CH_2^+ are similar. The analysis of the momentum correlation of the electrons and ions proves that an electron transfer process from CH_3 to the F^+ during the breakup of the molecule is responsible for the production of CH_2^+. Our results also show that Auger decay that happens at close internuclear distances provides information on the momentum of the core hole via the electronic Doppler shift of the electron. Even though this effect is theoretically difficult to describe, because it violates the Born-Oppenheimer approximation, it can be used as a tool for measuring charge redistribution during molecular dissociation.

The experiment was carried out with the approval of JASRI and was partly supported by the Japan Society of the Promotion of Science (JSPS) in the form of Grants-in-Aid for Scientific Research. The staff of SPring-8 are greatly acknowledged for providing an excellent experimental facility. C.M. and X.J.L. acknowledge JSPS for support.

[1] R. A. Marcus, Nobel Lecture, 1992.
[2] X. J. Liu, G. Prümper, E. Kukk, R. Sankari, M. Hoshino, C. Makochekanwa, M. Kitajima, H. Tanaka, Y. Yoshida, Y. Tamenori, and K. Ueda, Phys. Rev. A **72**, 042704 (2005).
[3] O. Kugeler, G. Prümper, R. Hentges, J. Viefhaus, D. Rolles, U. Becker, S. Marburger, and U. Hergenhahn, Phys. Rev. Lett. **93**, 033002 (2004).
[4] G. Prümper Y. Tamenori, A. DeFanis, U. Hergenhahn, M. Kitajima, M. Hoshino, H. Tanaka, and K. Ueda, J. Phys. B **38**, 1 (2005).
[5] P. Morin and I. Nenner, Phys. Rev. Lett. **56**, 1913 (1986).
[6] O. Björneholm, A. Ausmees, I. Hjelte, R. Feifel, H. Wang, C. Miron, M. N. Piancastelli, and S. Svensson, Phys. Rev. Lett. **84**, 2826 (2000).
[7] K. Ueda, M. Kitajima, A. De Fanis, T. Furuta, H. Shindo, H. Tanaka, K. Okdada, R. Feifel, S. L. Sorensen, H. Yoshida, and Y. Senba, Phys. Rev. Lett. **90**, 233006 (2003).
[8] M. Kitajima, K. Ueda, A. De Fanis, T. Furuta, H. Shindo, H. Tanaka, K. Okada, R. Feifel, S. L. Sorensen, F Gel'mukanov, A. Baev, and H. Ågren, Phys. Rev. Lett. **91**, 213003 (2003).
[9] G. Prümper, K. Ueda, U. Hergenhahn, A. De Fanis, Y. Tanemori, M. Kitajima, M. Hoshino, and H. Tanaka, J. Electron Spectrosc. Relat. Phenom. **144-147**, 227 (2005).
[10] H. Ohashi, E. Ishiguro, Y. Tamenori, H. Okamura, A. Hiraya, H. Yoshida, Y. Senba, K. Okada, N. Saito, I. H. Suzuki, K. Ueda, T. Ibuki, S. Nagaoka, I. Koyano, and T. Ishikawa, Nucl. Instrum. Methods Phys. Res. A **467-468**, 533 (2001).
[11] S. Svensson, L. Karsson, N. Mårtensson, P. Baltzer, and B.

Wannberg, J. Electron Spectrosc. Relat. Phenom. **50**, C1 (1990).

[12] K. Ueda, X. J. Liu, G. Prümper, H. Yoshida, D. Sasaki, M. Kitajima, T. Tanaka, C. Makochekanwa, M. Hoshino, and H. Tanaka, Chem. Phys. Lett. **413**, 263 (2005).

[13] G. Prümper, V. Carravetta, Y. Muramatsu, X. J. Liu, K. Ueda, Y. Tamenori, and M. Kitajima, in *Ionization, Correlation, and Polarization in Atomic Collisions*, edited by A. Lahman-Bennani and B. Lohmann, AIP Conf. Proc. No. 811 (AIP, Melville, NY, 2006), p. 144.

[14] G. Prümper, X. J. Liu, and K. Ueda, Radiat. Phys. Chem. **75**, 2019 (2006).

[15] C.-M. Liegener, Chem. Phys. Lett. **151**, 83 (1988).